

1 Supplementary Data

2

3

4

5 **Targeting cell surface glucose-regulated protein 94 in**
6 **gastric cancer with an anti-GRP94 human monoclonal**
7 **antibody**

8

9

10 Hyun Jung Kim^{1,#}, Yea Bin Cho^{2,#}, Kyun Heo^{1,2,3}, Ji Woong Kim¹, Ha Gyeong Shin¹,
11 Eun-bi Lee¹, Seong-Min Park⁴, Jong Bae Park⁴, Sukmook Lee^{1,2,3,*}.

12

13 ¹Department of Biopharmaceutical Chemistry, Kookmin University, Seoul, 02707, Republic
14 of Korea. ²Department of Chemistry, Kookmin University, Seoul, Republic of Korea.
15 ³Antibody Research Institute, Kookmin University, Seoul 02707, Republic of Korea.
16 ⁴Department of Cancer Biomedical Science, Graduate School of Cancer Science and Policy,
17 National Cancer Center, Goyang, Gyeonggi 10408, Republic of Korea

18

19

20 **Corresponding Author's Information:** Sukmook Lee, Tel: +82-2-910-6763; Fax:
21 +82-2-910-4115; E-mail: lees2018@kookmin.ac.kr.

22 MATERIALS AND METHODS

23 Immunohistochemistry

24 Immunohistochemistry (IHC) was performed as previously described with minor
25 modifications (1). Briefly, a total of 27 cancer tissue samples printed on tissue slides
26 (Supplementary Table. 1) were purchased from SuperBioChips Laboratories (Seoul,
27 Korea). The slides were initially incubated with a rabbit anti-GRP94 polyclonal
28 antibody (1:200; Abcam, Cambridge, UK), followed by OV HRP multimer.
29 Immunoreactive proteins were visualized using the OptiView DAB IHC Detection Kit
30 (Roche, Rotkreuz, Switzerland). Chromogenic reactions were initiated by incubating
31 the slides with a freshly prepared 3,3'-diaminobenzidine tetrahydrochloride (DAB)
32 solution. All samples were counterstained with hematoxylin. GRP94 expression was
33 observed using light microscopy on a Leica Aperio AT2 (Leica Biosystems, Wetzlar,
34 Germany).

35 Interpretation of immunohistochemical staining

36 A semi-quantitative approach was employed to interpret the immunohistochemical
37 staining of GRP94. The expression of GRP94 was calculated based on the intensity
38 values of DAB and hematoxylin obtained from six randomly selected fields of each
39 specimen. The staining intensity was rated on a scale of 1 (negative) to 4 (strong),
40 with 2 indicating weak and 3 indicating moderate staining. The extent of positive
41 staining in the tissue samples was assessed as follows: 0% - 9% was scored as none,
42 10% - 29% as 1, 30% - 39% as 2, 40% - 49% as 3, and 50% - 100% as 4. The density
43 value of GRP94 expression was measured using Image J software version Fiji
44 (National Institutes of Health, Bethesda, MD, USA). This approach provided a
45 comprehensive and objective assessment of GRP94 expression in the analyzed
46 tissue samples.

47 Cell culture

48 All cells were maintained at 37 °C with 5% CO₂ unless specified otherwise. Human
49 gastric cancer (GC; MKN45, AGS, NCI-N87, and KATO III) and liver cancer (LC; Huh-
50 7) cell lines were maintained in Roswell Park Memorial Institute 1640 medium

51 (Gibco, Billings, MT, USA) supplemented with 10% (v/v) fetal bovine serum (FBS,
52 Gibco) and 1% (v/v) penicillin/streptomycin (Gibco). Human LC cell lines (Hep G2
53 and SK-HeP-1) were cultured in Dulbecco's Modified Eagle's Medium (Gibco) with
54 the same supplements. Expi293F cells were cultured in the Expi293 expression
55 medium (Gibco) in a humidified shaking incubator at 37 °C with 8% CO₂.

56 **Overexpression and purification of K101.1**

57 K101.1 was produced as previously described (2). Briefly, a bicistronic mammalian
58 expression vector encoding K101.1 was transfected into suspension-adapted
59 Expi293™ cells using the Expi293 transfection kit (Thermo Fisher Scientific,
60 Waltham, MA, USA), following the manufacturer's instructions. Seven days after
61 transfection, the overexpressed IgG was purified from the culture media using
62 affinity column chromatography with Protein A Sepharose® (Repligen, Waltham,
63 MA, USA). Following purification and subsequent dialysis in phosphate-buffered
64 saline (PBS), the purity of the IgG antibody was assessed by sodium dodecyl
65 sulfate-polyacrylamide gel electrophoresis and Coomassie Brilliant Blue staining.

66 **Flow cytometry**

67 To confirm the expression of GRP94 on the cell surface, 2×10^5 human gastric (NCI-
68 N87, AGS, MKN45, and KATO III) and liver (Hep G2, Huh-7, and SK-HeP-1) cancer
69 cells were fixed with 4% (w/v) paraformaldehyde (PFA), blocked with PBS
70 containing 1% (w/v) bovine serum albumin (BSA), and stained with a rabbit anti-
71 GRP94 polyclonal antibody (1:100; Abcam) for 1 h. Additionally, the cells were
72 incubated with Alexa Fluor 488-labeled anti-rabbit IgG (1:1000; Invitrogen,
73 Carlsbad, CA, USA) for 1 h.

74 To confirm the specific binding of K101.1 to the GC cell surface GRP94, 40 µg/mL of
75 rhGRP94 was preincubated with 4 µg/mL of K101.1 in PBS for 3 h at room
76 temperature. Then, NCI-N87 cells fixed with 4% PFA were incubated with these
77 mixtures for 1 h at room temperature. Following several washes with PBS
78 containing 1% BSA, the cells were incubated with Alexa Fluor 488-labeled anti-
79 human Fc IgG (Invitrogen, 1:200) for 1 h at room temperature in the dark. The

80 fluorescence intensity was measured using flow cytometry (Millipore, Burlington,
81 MA, USA).

82 To evaluate the effect of K101.1 on the downregulation of cell surface GRP94, NCI-
83 N87 cells (2×10^5 cells) were fixed with 4% (w/v) PFA. The fixed and unfixed cells
84 were washed twice with PBS containing 1% (w/v) BSA and incubated in the
85 presence or absence of 20 g/ml K101.1 for 4 h at 37 °C. The cells were stained with
86 rabbit anti-GRP94 polyclonal antibody (Abcam) for 2 h at 4 °C. Subsequently, the
87 cells were washed three times with PBS containing 1% (w/v) BSA, incubated with
88 Alexa Fluor 488-labeled anti-rabbit IgG (1000:1; Invitrogen), and analyzed using
89 flow cytometry (Millipore).

90 **Public RNA-seq data analysis**

91 Public RNA-seq data containing clinical information were obtained from the
92 International Cancer Genome Consortium (ICGC) data portal. Specifically, we
93 downloaded the stomach adenocarcinoma (STAD) RNA-seq data and clinical
94 information from release 28. Our analysis focused on assessing the expression of
95 GRP94 mRNA, using 35 samples from normal gastric tissues and 413 samples from
96 GC tissues. To determine mRNA expression levels, we utilized the normalized read
97 counts, which were calculated using the ICGC RNA-seq pipeline. Graphs were
98 generated using the R program.

99 **In Vitro measurement of GC cell growth**

100 To examine the effect of K101.1 on GC cell growth, NCI-N87 cells were seeded into
101 96-well plates (3×10^4 cells/well) and then treated with 20 µg/ml control IgG and
102 K101.1 for 60 h. Cell growth was assessed using the Cell Counting Kit-8 (Sigma-
103 Aldrich, St. Louis, MO, USA) according to the manufacturer's instructions. The final
104 absorbance was measured at 450 nm using a microplate reader (Synergy H1, BioTek,
105 Winooski, VT, USA).

106 **Measurement of antibody internalization**

107 Antibody internalization in NCI-N87 cells was assessed using the FabFluor-pH Red

108 Antibody Labeling Reagent (Sartorius, Göttingen, Germany) following the
109 manufacturer's instructions. The FabFluor reagent exhibits very low fluorescence
110 intensity under neutral or basic pH conditions (on the cell surface or outside the cell).
111 However, its fluorescence intensity increases in the acidic conditions of the
112 endosomal and lysosomal compartments upon internalization of the reagent-
113 labeled antibody. NCI-N87 cells were seeded at a density of 1×10^4 cells per well in
114 96-well culture plates and allowed to adhere overnight. Control IgG and K101.1
115 antibodies were separately labeled with the human FabFluor-pH Red Antibody
116 Labeling Reagents at a molar ratio of 1:3 in PBS. The cells were then incubated for
117 15 min. Subsequently, the plates were transferred to the IncuCyte SX1 Live Cell
118 Analysis instrument (Sartorius), and images were captured using a 10x objective
119 over a 12-h period to measure fluorescence intensities.

120 **Cell enzyme-linked immunosorbent assay**

121 To assess the effect of K101.1 on GRP94 downregulation on the surface of NCI-N87
122 GC cells, 3×10^4 NCI-N87 cells were plated on a 96-well plate and incubated with
123 20 $\mu\text{g/ml}$ of either control IgG or K101.1 for 0, 2, 4, 6, or 12 h at 37 °C. Subsequently,
124 the cells were washed with ice-cold PBS and fixed with PBS containing 4% (w/v)
125 PFA. Following fixation, the cells were incubated with a rabbit anti-GRP94 polyclonal
126 antibody (1:5000, Abcam). After three washes with ice-cold PBS, the plates were
127 further incubated with HRP-conjugated anti-rabbit Fc secondary antibody (1:5000;
128 Invitrogen) for 1 h at 37 °C. Following another three washes with ice-cold PBS,
129 3,3',5,5'-tetramethylbenzidine (TMB) substrate solution was added. The optical
130 density was measured at 450 nm using a microplate reader (Synergy H1, BioTek)
131 after quenching with 1 M H_2SO_4 solution.

132 ***In vivo* efficacy testing**

133 The animals were maintained in a specific pathogen-free environment and
134 acclimated to the laboratory conditions for at least one week before the experiment.
135 The housing and care of the mice were carried out at the National Cancer Center's
136 accredited animal facility (unit number NCC-22-849) in accordance with the
137 AAALAC International Animal Care Policy. To assess the impact of K101.1 on NCI-

138 N87 tumor growth, BALB/c-nude mice were subcutaneously injected with 1×10^7
139 NCI-N87 cells. Once the tumor volume reached approximately 100 mm^3 , the mice
140 ($n = 14$) were randomly divided into groups and administered intravenous injections
141 of PBS and 10 mg/kg of K101.1, as well as intraperitoneal injections of 40 mg/kg of
142 5-fluorouracil (5-FU) (Sigma-Aldrich) twice a week for three weeks. The mice were
143 weighed, and tumor sizes were measured once a week, up to day 23.

144 ***In vivo* toxicity testing**

145 To assess *in vivo* toxicity, established procedures were followed. Briefly, BALB/c-
146 nude mice ($n = 8$) received intravenous injections of 10 mg/kg K101.1 or
147 intraperitoneal injections of 40 mg/kg 5-FU, twice weekly. The mice's body weights
148 were recorded weekly throughout the 23-day study period. At the end of the study,
149 the mice were euthanized, and blood samples were collected. Enzymatic activities,
150 including glutamate oxaloacetate transaminase (GOT), glutamate pyruvate
151 transaminase (GPT), total bilirubin (TBIL), blood urea nitrogen (BUN), and
152 creatinine (CRE), were analyzed using a Fuji Dri-Chem 3500 biochemistry analyzer
153 (Fujifilm, Tokyo, Japan).

154 ***In vivo* fluorescence IHC**

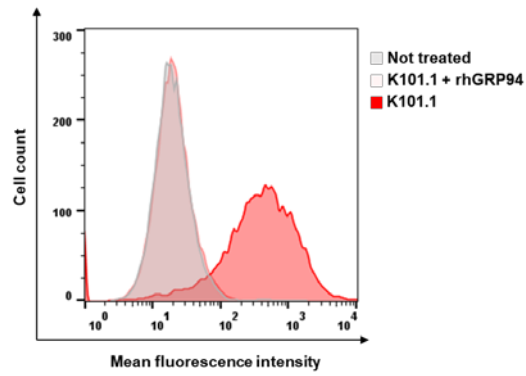
155 Resected tumor specimens were embedded in an optimal cutting temperature (OCT)
156 compound (Sakura Finetek Japan Co., Ltd., Tokyo, Japan) and stored at -80°C . For
157 IHC, frozen blocks were sectioned into $10\text{-}\mu\text{m}$ slices using a cryostat microtome
158 (Thermo Fisher Scientific). These sections were fixed in 4% PFA in PBS for 10 min
159 and washed three times with PBS. To assess the impact of K101.1 on microvessel
160 density (MVD), tissue sections were blocked with 20% FBS in PBS for 30 min.
161 Subsequently, the sections were incubated with an anti-CD31 monoclonal antibody
162 (R&D Systems, Minneapolis, MN, USA) for 1 h. After three PBS washes, the sections
163 were further incubated with FITC-conjugated anti-rat IgG (Invitrogen) for 1 h. To
164 investigate the efficacy of K101.1 on apoptosis, each tissue section was subjected
165 to individual examination of apoptosis and nuclear morphology using terminal
166 deoxynucleotidyl transferase-mediated dUTP nick end labeling (TUNEL; Roche)
167 and 4',6-diamidino-2-phenylindole, dihydrochloride (DAPI; Sigma-Aldrich)

168 staining. Fluorescence images were captured using a confocal laser scanning
169 microscope (Leica biosystems). Furthermore, MVD and apoptosis rates were
170 quantified using inForm Advanced Image Analysis Software (PerkinElmer, Waltham,
171 MA, USA) and LASX software (Leica), respectively.

172 **Statistical analysis**

173 The data were analyzed using GraphPad Prism 7.0 (GraphPad Software Inc., La Jolla,
174 CA, USA). Two-tailed Student's *t*-tests were used for comparisons between two
175 groups, and a two-way analysis of variance (ANOVA) with Bonferroni's correction
176 was applied for multiple comparisons. All data are presented as means \pm standard
177 errors of the mean (SEM). Differences with *P* values below 0.05 were considered
178 statistically significant and indicated on the graphs using the following symbols: * *P*
179 < 0.05 , ** *P* < 0.01 , *** *P* < 0.001 .

180



181

182 **Supplementary Fig. 1.** Specific binding of K101.1 to cell surface GRP94 on NCI-N87
183 cells. The specific binding of K101.1 to cell surface GRP94 on NCI-N87 cells was
184 investigated using flow cytometry under different conditions. The analysis was
185 performed in the absence of K101.1 (gray), in the presence of K101.1 (red), or in
186 the presence of K101.1 preincubated with rhGRP94 (light red).

187 **Supplementary Table. 1.** Detailed information regarding cancer tissue samples
 188 printed on the tissue microarray

189	Organ	Diagnosis	Age	Sex
190	Skin	squamous cell carcinoma	65	M
191	Subcutis	Liposarcoma	36	M
192	Breast	infiltrating duct carcinoma	58	F
193	Lymph node	Hodgkin lymphoma	34	F
194	Bone	Osteosarcoma	54	F
195	Lung	Adenocarcinoma	61	M
196	Lung	squamous cell carcinoma	72	M
197	Liver	Cholangiocarcinoma	41	F
198	Liver	hepatocellular carcinoma	54	M
199	Liver	metastatic adenocarcinoma (from rectum)	52	M
200	Esophagus	squamous cell carcinoma	77	M
201	Gastric	Adenocarcinoma	65	F
202	Gastric	malignant lymphoma, diffuse large B cell	53	M
203	Gastric	signet ring cell carcinoma	40	F
204	Duodenum	gastrointestinal stromal tumor, malignant	61	M
205	Colorectal	Adenocarcinoma	62	M
206	Colorectal	Adenocarcinoma	73	M
207	Kidney	renal cell carcinoma	57	M
208	Bladder	invasive urothelial carcinoma	65	M
209	Prostate	Adenocarcinoma	63	M
	Testis	Seminoma	35	M
	Uterine	squamous cell carcinoma	65	F
	Uterine	Adenocarcinoma	69	F
	Ovary	metastatic adenocarcinoma (from stomach)	44	F
	Ovary	mucinous cystadenocarcinoma	15	F
	Ovary	serous cystadenoma of low malignant potential	44	F
	Thyroid	papillary carcinoma	69	F

210 **REFERENCES**

- 211 1. Kim MR, Jang JH, Park CS et al (2017) A Human Antibody That Binds to the Sixth
212 Ig-Like Domain of VCAM-1 Blocks Lung Cancer Cell Migration In Vitro. *Int. J. Mol.*
213 *Sci.* 18, 566
- 214
- 215 2. Cho YB, Kim JW, Heo K et al (2022) An internalizing antibody targeting of cell
216 surface GRP94 effectively suppresses tumor angiogenesis of colorectal cancer.
217 *Biomed. Pharmacother.* 150, 113051

218

219